Supporting Information

A Cost-Effective Alpha-Fluorinated Bithienyl Benzodithiophene Unit for High-Performance Polymer Donor Material

Wenqing Zhang[a], *Chenkai Sun*[a,e]*, *Shucheng Qin*[b,c], *Ziya Shang*[b,c], *Shaman Li*[c], *Can Zhu*[b,c], *Guang Yang*[a], *Lei Meng*[b,c]*, *Yongfang Li*[b,c,d]*

[a] College of Chemistry, and Green Catalysis Center, Zhengzhou University, Zhengzhou 450001, China

[b] Beijing National Laboratory for Molecular Sciences, CAS Key Laboratory of Organic Solids, Institute of Chemistry, Chinese Academy of Sciences, Beijing 100190, China

[c] School of Chemical Science, University of Chinese Academy of Sciences, Beijing 100049, China.

[d] Laboratory of Advanced Optoelectronic Materials, College of Chemistry, Chemical Engineering and Materials Science, Soochow University, Suzhou 215123, China

[e] Key Laboratory of Organic Synthesis of Jiangsu Province, College of Chemistry, Chemical Engineering and Materials Science, Soochow University, Suzhou, 215123, China

* Corresponding authors

E-mail: schenkai@zzu.edu.cn (Chenkai Sun), menglei@iccas.ac.cn (Lei Meng), liyf@iccas.ac.cn (Yongfang Li)

Materials and synthesis

The electron acceptors Y6 and ICBA are purchased from Solarmer Materials Inc and J&K, respectively. Other chemicals and solvents are obtained from J&K, Alfa Aesar, and TCI Chemical Co., etc. All the reagents and commercial compounds are used as received. The synthetic routes of PBQ10 and α-PBQ10 are shown in **Scheme 1**. The compounds 4-7, monomer BDTT-F, monomer 9, and polymer PBQ10 are synthesized according to the reported literatures.[1-4] The synthetic details of compound 2, compound 3, monomer α-BDTT-F and polymer α-PBQ10 are described in the Experimental Section.

General Characterization

^{1}H NMR and ^{13}C NMR spectra of the corresponding compounds are measured on a Bruker DMX-400 spectrometer using *d*-chloroform as solvent and trimethylsilane as the internal reference. Gel permeation chromatography (GPC) measurements are performed on Agilent PL-GPC 220 instrument with high temperature chromatograph, using 1,2,4-trichlorobenzene as the eluent at 160 °C. UV-visible absorption spectra are measured on a Hitachi U-3010 UV-vis spectrophotometer. Electrochemical cyclic voltammetry is performed on a Zahner IM6e Electrochemical Workstation under a nitrogen atmosphere using three-electrode system with a Pt disk working electrode, an Ag/AgCl reference electrode and a Pt wire counter electrode in acetonitrile solution of tetrabutylammonium hexafluorophosphate (Bu_4NPF_6), and ferrocene/ferrocenium (Fc/Fc^+) redox couple is used as an internal reference. Transmission electron microscope (TEM) measurement was performed on the JEM-ARM2100F Transmission Electron Microscope, with samples prepared under the same condition of the optimal photoactive layer on PEDOT: PSS layer of the devices. Atomic force microscope (AFM) measurement was performed on the Bruker-ICON2-SYS atomic force microscope with samples prepared under the same condition of the optimal photoactive layer on PEDOT: PSS layer of the devices.

Measurement of charge carrier mobilities

The charge carrier mobilities were measured with the device structure of

ITO/PEDOT:PSS/active layer/MoO_3/Ag for hole mobility and ITO/ZnO/active layer/PDINN/Ag for electron mobility. The hole and electron mobilities are calculated according to the space-charge-limited current (SCLC) method equation:

$$J = \frac{9\varepsilon_0\varepsilon_r\mu V^2}{8L^3} \qquad \text{(S1)}$$

Where J is the current density, ε_0 is the dielectric constant of empty space, ε_r is the relative dielectric constant of active layer materials which is usually 2-4 for organic semiconductors, herein we use a relative dielectric constant of 3, μ is the charge mobility, V is the internal voltage in the device, and $V = V_{appl}-V_{bi}-V_s$, where V_{appl} is the voltage applied to the devices, and V_{bi} is the built-in voltage resulting from the relative work function difference between the two electrodes (in the hole-only device, the V_{bi} value is 0.2 V), V_s is the voltage drop from the series resistance and L is the thickness of the active layers.

Device fabrication and characterization

The PSCs were fabricated with a structure of ITO/PEDOT:PSS/active layer/PDINN/Ag. The ITO glass was cleaned by sequential ultrasonic treatment in detergent, deionized water, acetone and isopropanol. Then the dried ITO glass was treated with an ultraviolet-ozone chamber (Ultraviolet Ozone Cleaner, Jelight Company, USA) for 25 min. A thin layer of PEDOT: PSS was prepared on precleaned ITO glass through spin-coating a PEDOT: PSS aqueous solution (Baytron P VP AI 4083 from H. C. Starck) at 5000 rpm and dried subsequently at 150 °C for 20 min in the air. The substrates were then transferred into a N_2-filled glovebox. A blend solution was prepared by dissolving the donor and acceptor in chloroform ($CHCl_3$), and then the blend solution was spin-coated at 3000 rpm onto the PEDOT:PSS layer. After spin-coating, the active layers were annealed at 85 °C for 10 min. Then, methanol solution of PDINN at a concentration of 1.0 mg mL^{-1} is prepared upon the active layer by spin-coating at 3000 rpm to afford a PDINN cathode buffer layer. Finally, cathode metal Ag was deposited at a pressure of 1.0×10^{-6} Pa. The active layer effective area of the devices was 4.7 mm^2, which is defined using an optical microscope (Olympus BX51). The current density-voltage (*J-V*) characteristics of the PSCs were measured in a nitrogen glove box with a Keithley 2450 Source Measure unit. Oriel Sol3A Class AAA Solar Simulator (model, Newport 94023A) with a 450W xenon lamp

and an air mass (AM) 1.5 filter was used as the light source. The light intensity was calibrated to 100 mW cm^{-2} by a Newport Oriel 91150V reference cell. The input photon to converted current efficiency (IPCE) was measured by Solar Cell Spectral Response Measurement System QE-R3-011 (Enli Technology Co., Ltd., Taiwan). The light intensity at each wavelength was calibrated with a standard single-crystal Si photovoltaic cell.

DFT calculation

All calculations are performed by ORCA (*version 4.2.1*) unless otherwise statement. The conformations are generated by molclus (*version 1.9.4*) and optimized by DFT calculation with a function of wB97X-D3 with a basis set of def2-TZVP. The straight and branched alkyl chains were simplified to methyl and isobutyl, respectively, for saving time. The single point energies and gradients were further calculated with wB97M-V function, the energy levels were calculated with B3LYP function, the dipole moments were calculated with PBE0 function, the basis set were all with def2-TZVP.[5,6] The molecular orbitals and geometries were analyzed by Multiwfn (*version 3.6*) and VMD (*version 1.9.3*) for visualization.[7,8]

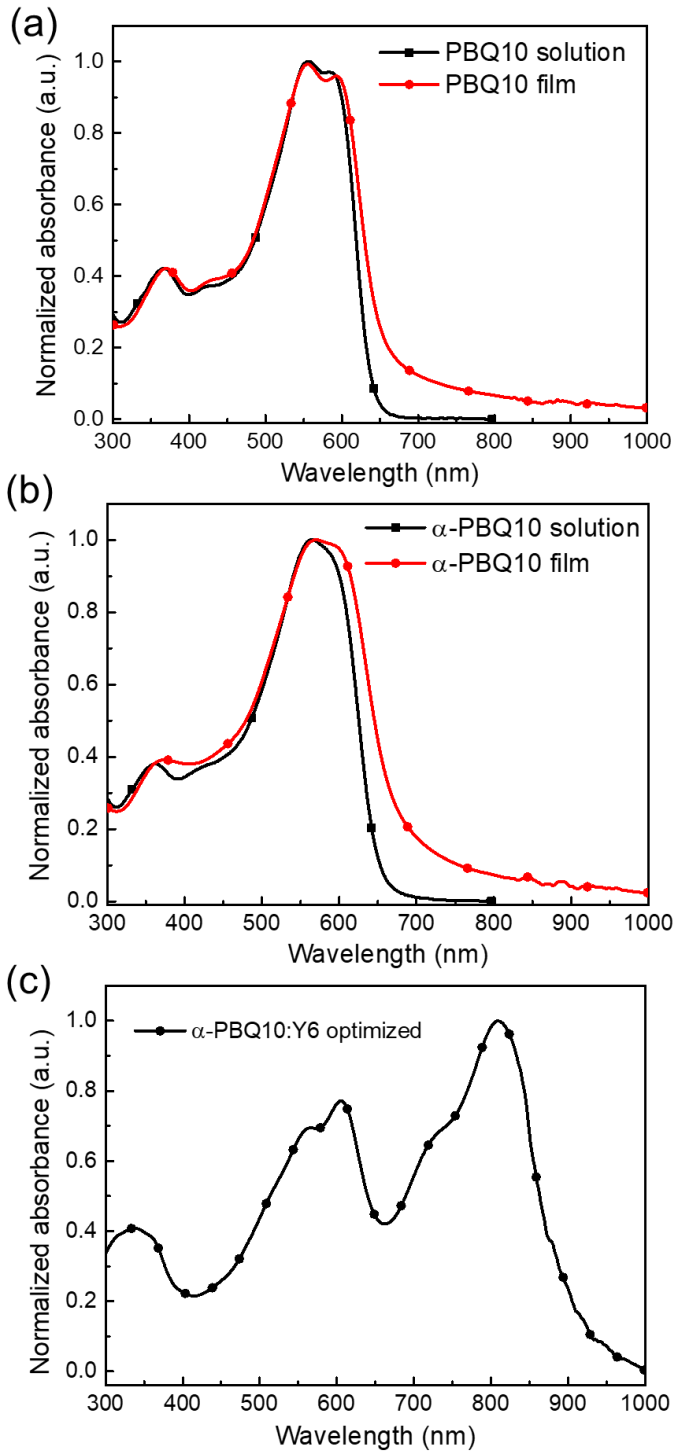

Figure S1. Normalized absorption spectra of (a) polymer PBQ10 in the solution and in the film, (b) polymer α-PBQ10 in the solution and in the film and (c) α-PBQ10:Y6 film (optimized with 0.5% CN and thermal annealing treatment).

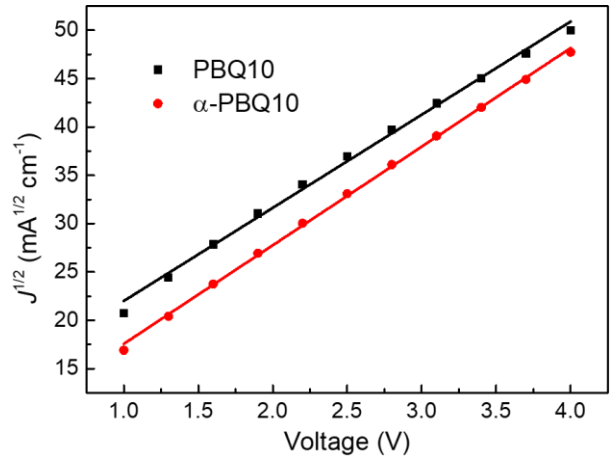

Figure S2. $J^{1/2}$~V ($V = V_{appl}$-V_{bi}-V_s) characteristics of the hole-only devices based on polymers PBQ10 and α-PBQ10.

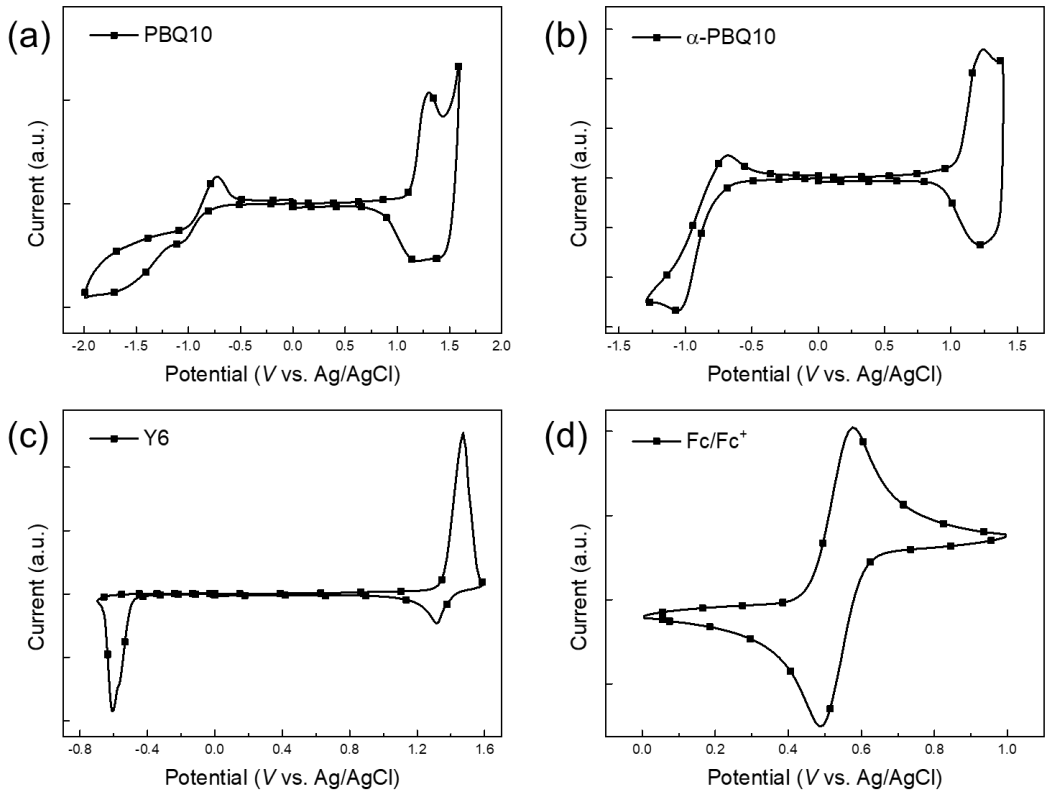

Figure S3. Cyclic voltammograms of (a) the polymer PBQ10, (b) the polymer α-PBQ10, (c) electron accepter Y6, and (d) Fc/Fc^+ measured in 0.1 mol L^{-1} Bu_4NPF_6 acetonitrile solution at a scan rate of 20 mV s^{-1}.

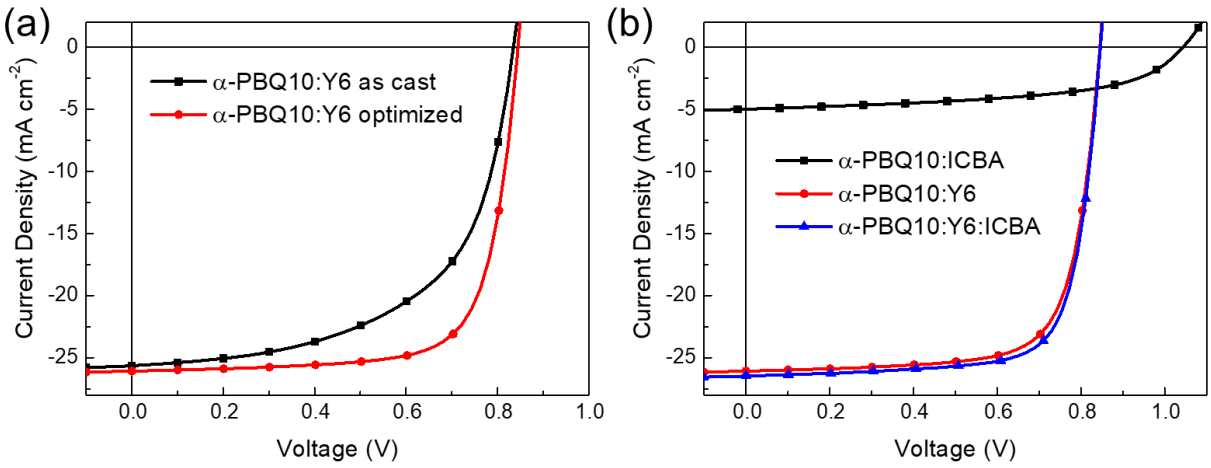

Figure S4. *J-V* curves of the devices based on (a) α-PBQ10:Y6 (as cast and optimized with 0.5% CN and thermal annealing treatment), (b) α-PBQ10:ICBA, α-PBQ10:Y6 and α-PBQ10:Y6:ICBA.

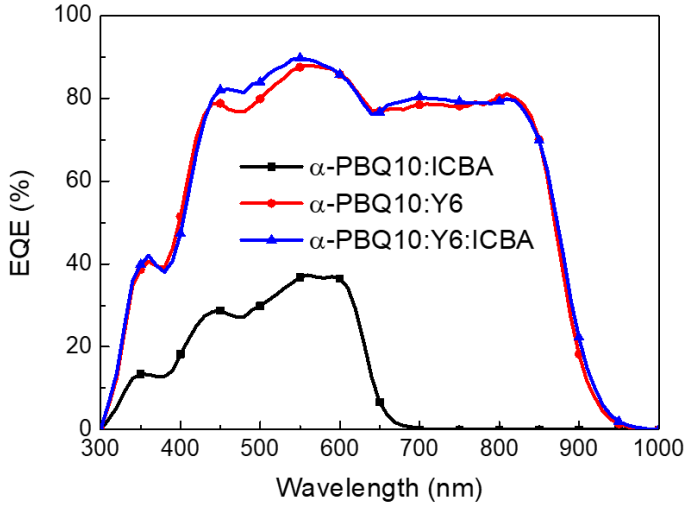

Figure S5. EQE spactra of the devices based on α-PBQ10:ICBA, α-PBQ10:Y6 and α-PBQ10:Y6:ICBA.

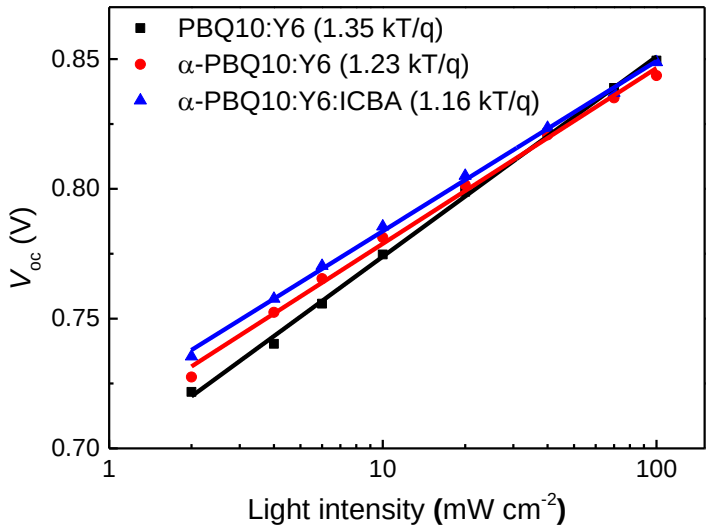

Figure S6. Dependence of V_{oc} on P_{light} of the binary and ternary devices.

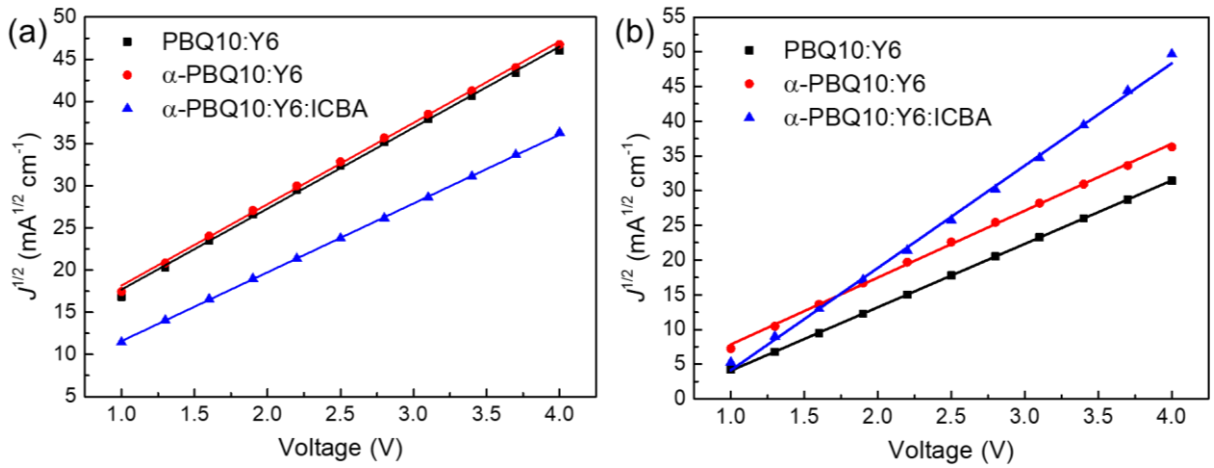

Figure S7. $J^{1/2}$~V (V = V_{appl}-V_{bi}-V_s) characteristics of the (a) hole-only devices based on PBQ10:Y6, α-PBQ10:Y6 and α-PBQ10:Y6:ICBA (b) electron-only devices based on PBQ10:Y6, α-PBQ10:Y6 and α-PBQ10:Y6:ICBA.

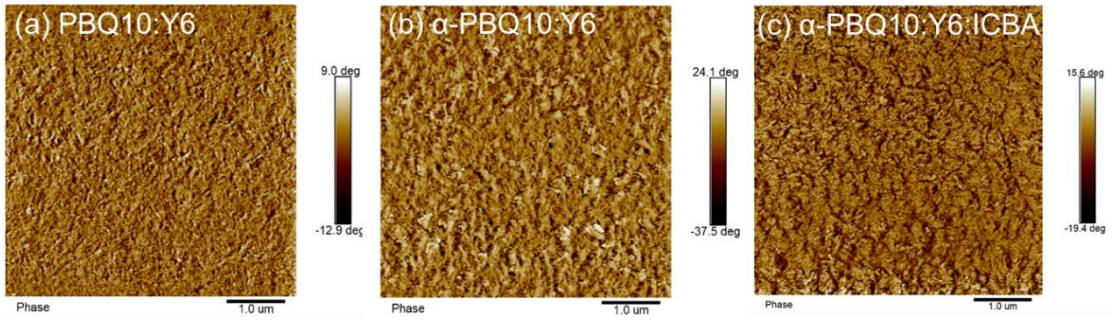

Figure S8. AFM phase images of (a) the PBQ10:Y6 blend, (b) the α-PBQ10:Y6 blend , and (c) the α-PBQ10:Y6:ICBA blend.

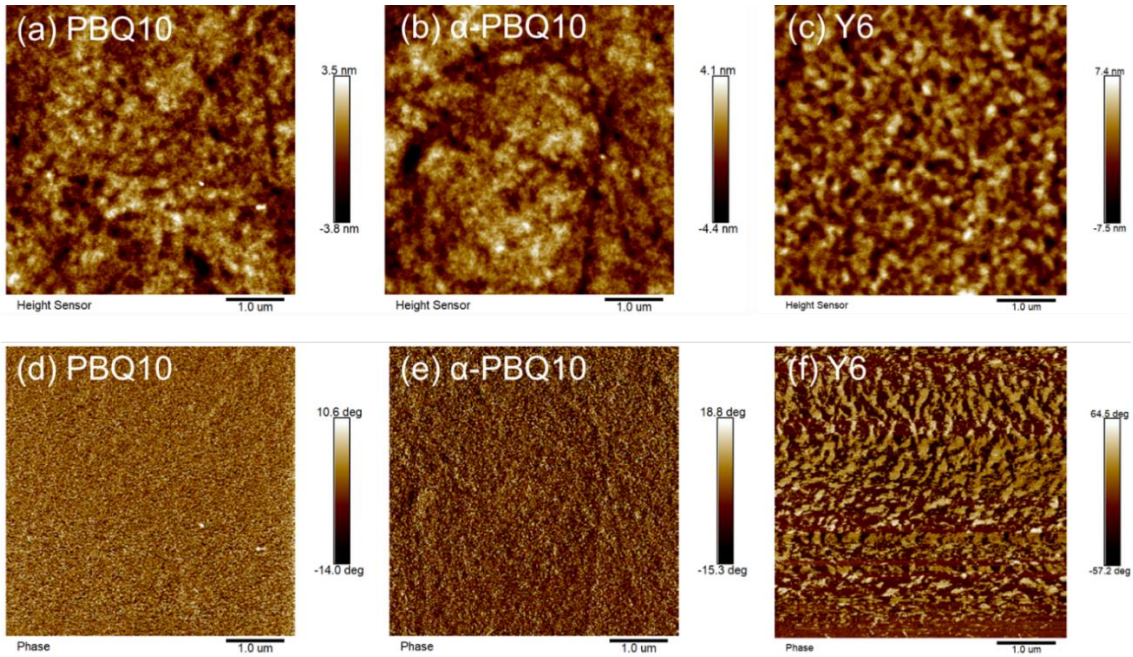

Figure S9. AFM (a-c) height images and (d-f) phase images of the PBQ10, α-PBQ10 and Y6.

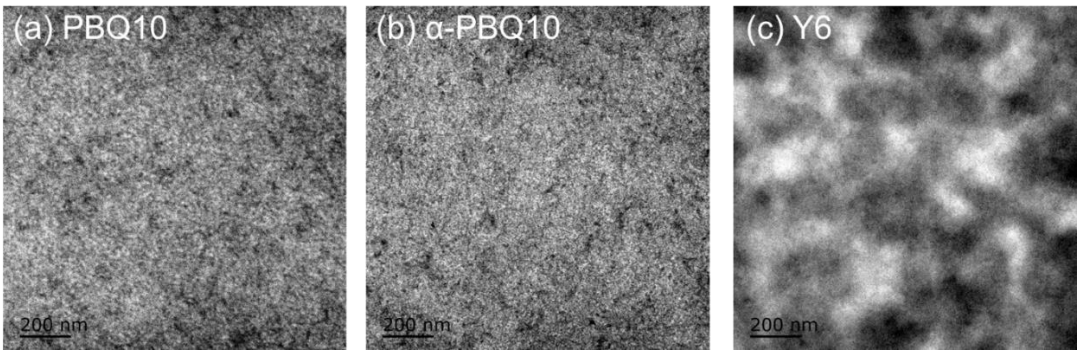

Figure S10. TEM images of (a) PBQ10, (b) α-PBQ10, and (c) Y6.

Table S1. Photovoltaic performance parameters of the PSCs based on α-PBQ10:Y6 with different D: A weight ratio under the illumination of AM 1.5G, 100 mW cm^{-2}.

D/A ratios	V_{oc} (V)	J_{sc} (mA cm^{-2})	FF (%)	PCE (%)
1:1	0.843	25.65	70.95	15.34
1:1.2	0.845	26.12	73.65	16.26
1:1.5	0.839	25.16	67.67	14.28

Table S2. Photovoltaic performance parameters of the PSCs based on α-PBQ10:Y6 with different 1-CN additive volume ratio under the illumination of AM 1.5G, 100 mW cm^{-2}.

CN (vol %)	V_{oc} (V)	J_{sc} (mA cm^{-2})	FF (%)	PCE (%)
0	0.845	25.36	58.16	12.46
0.3	0.842	25.43	66.61	14.26
0.5	0.845	26.12	73.65	16.26
0.7	0.832	25.30	73.33	15.43

Table S3. Photovoltaic performance parameters of the PSCs based on α-PBQ10:Y6 with different annealing temperature for 10 min under the illumination of AM 1.5G, 100 mW cm^{-2}.

annealing temperature (°C)	V_{oc} (V)	J_{sc} (mA cm^{-2})	FF (%)	PCE (%)
70	0.847	24.99	71.10	15.04
85	0.845	26.12	73.65	16.26
100	0.821	25.91	73.87	15.71
110	0.815	26.18	71.85	15.33

Table S4. Photovoltaic performance parameters of the α-PBQ10:Y6:ICBA based PSCs with different ICBA weight ratios under the illumination of AM 1.5G, 100 mW cm^{-2}.

α-PBQ10:Y6:ICBA	V_{oc} (V)	J_{sc} (mA cm^{-2})	FF (%)	PCE (%)
1:1.2:0.15	0.846	26.45	74.96	16.77
1:1.2:0.3	0.851	25.46	73.03	15.82
1:1.2:0.4	0.842	24.94	71.92	15.10
1:1:0.2	0.857	24.22	71.10	14.75

Table S5. The hole (μ_h) and electron (μ_e) mobilities of the binary and ternary PSCs.

Device	μ_h ($cm^2 V^{-1} s^{-1}$)	μ_e ($cm^2 V^{-1} s^{-1}$)	μ_h/μ_e
PBQ10:Y6	5.32×10^{-4}	3.71×10^{-4}	1.43
α-PBQ10:Y6	5.38×10^{-4}	4.14×10^{-4}	1.29
α-PBQ10:Y6:ICBA	5.48×10^{-4}	5.30×10^{-4}	1.03

References

(1) Zhang, M.; Guo, X.; Ma, W.; Ade, H.; Hou, J. A Large-Bandgap Conjugated Polymer for Versatile Photovoltaic Applications with High Performance. *Adv. Mater*. **2015**, *27*, 4655-4660.

(2) Huang, J.; Peng, R.; Xie, L.; Song, W.; Hong, L.; Chen, S.; Wei, Q.; Ge, Z. A Novel Polymer Donor Based on Dithieno[2,3-*d*:2′,3′-*d*″]benzo[1,2-*b*:4,5-*b*′]dithiophene for Highly Efficient Polymer Solar Cells. *J. Mater. Chem. A* **2019**, *7*, 2646-2652.

(3) Xu, S.; Wang, X.; Feng, L.; He, Z.; Peng, H.; Cimrova, V.; Yuan, J.; Li, Y.; Zou, Y. Optimizing Conjugated Side Chains on Quinoxaline Based Polymers for Nonfullerene Solar Cells with 10.5% Efficiency. *J. Mater. Chem. A* **2018**, 6, 3074-3083.

(4) Sun, C.; Pan, F.; Qiu, B.; Qin, S.; Chen, S.; Shang, Z.; Meng, L.; Yang, C.; Li, Y. D-A Copolymer Donor Based on Bithienyl Benzodithiophene D-Unit and Monoalkoxy Bifluoroquinoxaline A-Unit for High-Performance Polymer Solar Cells. *Chem. Mater*. **2020**, *32*, 3254-3261.

(5) Weigend, F.; Ahlrichs, R. Balanced Basis Sets of Split Valence, Triple Zeta Valence and Quadruple Zeta Valence Quality for H to Rn: Design and Assessment of Accuracy. *Phys. Chem. Chem. Phys.* **2005**, *7*, 3297-3305.

(6) Weigend, F. Accurate Coulomb-Fitting Basis Sets for H to Rn. *Phys. Chem. Chem. Phys.* **2006**, *8*, 1057-1065.

(7) Humphrey, W.; Dalke, A.; Schulten, K. VMD: Visual Molecular Dynamics. *J. Mol. Graphics* **1996**, *14*, 33-38.

(8) Lu, T.; Chen, F. Multiwfn: A Multifunctional Wavefunction Analyzer. *J. Comput. Chem*. **2012**, *33*, 580-592.